Synthesis Techniques for High Performance Octave Bandwidth 180° Analog Phase Shifters

Stepan Lucyszyn, *Member, IEEE,* and Ian D. Robertson, *Member, IEEE*

Abstract—**Novel techniques for synthesizing 180° analog reflection-type phase shifters, with ultra-low phase and amplitude error characteristics, over a very wide bandwidth, are presented. The novel approach of cascading stages, where the nonlinear performance of each stage compliments those of the others, results in a significant advance in the linearity performance of traditional reflection-type phase shifters. In this paper, it is shown by theoretical analysis that three conditions must be satisfied by the reflection terminations, in order to achieve the desired response. The theoretical conditions and subsequent design equations are given. Simulation results for a 2-stage *Ku*-band cascaded-match reflection-type phase shifter show that a very low maximum phase error and amplitude error of ±2.4° and ±0.21 dB, respectively, can be achieved over a full octave bandwidth. Since the complexity of the overall topology is reduced to a minimum, the device appears insensitive to process variations and ideal for both hybrid and MMIC technologies.**

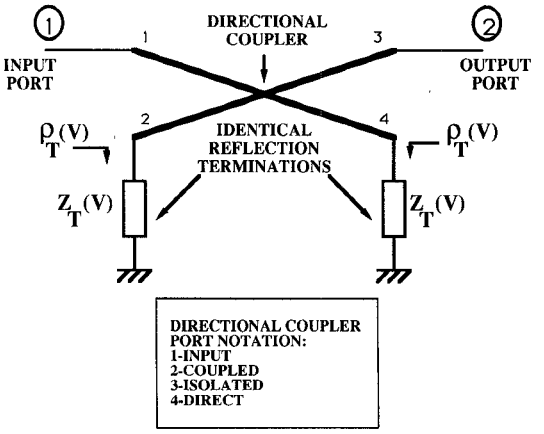

Fig. 1. Ideal 1-stage reflection-type phase shifter.

I. Introduction

THE reflection-type phase shifter (RTPS) was first introduced more than three decades ago by Hardin [1]. With reference to Fig. 1, a directional coupler produces incident voltage waves at the coupled and direct ports. These waves are reflected by identical impedances, Z_T, terminating the ports. The resulting reflected waves then combine at the input and isolation ports. If lossless reflection terminations are connected to an ideal 3 dB quadrature directional coupler, the resulting voltage wave vectors at the input port cancel each other out, while those at the isolation port re-enforce each other. In other words, all the power entering the input port will emerge from the isolation port. If the reflection terminations have a voltage dependent reactance, in the form of varactor-type devices or active inductors, the relative phase difference between the output voltage wave vector and the input voltage wave vector can be electronically varied, therefore, creating a relative shift in the phase angle of the overall voltage transmission coefficient.

Hardin proposed a simple series-tuned circuit for the reflection terminations, incorporating a single varactor diode in each. The resulting frequency response of the relative phase shift has a single hump. This hump can produce a maximum bandwidth of approximately 5–10%, for a phase error of ±5° between a 0° and 180° relative phase shift. This idea was further developed by Searing [2] and Garver [3] without much improvement to the bandwidth. Attempts to widen the bandwidth were proposed by Henoch *et al.* [4] and Ulriksson [5]. Here a parallel resonance mode was synthesized in the reflection termination—by connecting two series-tuned circuits, with different resonant frequencies, in parallel. A transmission line was then inserted between the reflection termination and the circulator directional coupler, in order to produce a double humped frequency response. This technique can increase the bandwidth by a factor of two. Also, the component values of the reflection terminations could only be determined by intensive optimization and human judgement. In recent years, a number of variations to the basic reflection terminations have been reported without significant advances in the phase shifter's overall performance [6]–[12].

A novel method for increasing the bandwidth is to combine the simplicity of Hardin's approach with the type of rippled frequency response produced by the latter approaches. Here, the phase shifter is split-up into matched cascaded stages. In order to achieve a full octave bandwidth, the optimum number of stages required by this cascaded-match reflection-type phase shifter (CMRTPS) is two; while a three stage design may be required to achieve a decade bandwidth. An ideal 2-stage CMRTPS is illustrated in Fig. 2.

For a 2-stage design each stage is similar to the one proposed by Hardin, except that the resonant frequency of the series-tuned reflection termination of the second

Manuscript received May 9, 1991; revised September 20, 1991.

The authors are with the Communications Research Group, Department of Electronic and Electrical Engineering, King's College, University of London, Strand, London, WC2R 2LS, England.

IEEE Log Number 9106049.

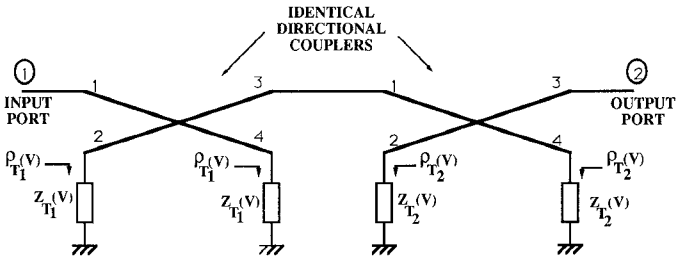

Fig. 2. Ideal 2-stage cascaded-match reflection-type phase shifter.

stage, ω_{OS_2} is always much greater then that of the first stage, ω_{OS_1}.

For a voltage-controlled phase shifter, the relative phase shift, $\Delta \angle S_{21}(\omega, V)|_{PS}$, can be defined as follows:

$$\Delta \angle S_{21}(\omega, V)|_{PS} = \angle\left(\frac{S_{21}(\omega, V)|_{PS}}{S_{21}(\omega, 0)|_{PS}}\right)$$

where

V = applied bias potential and $V_1 \leq V \leq V_2$

V_1 = minimum applied bias potential ($V_1 = 0$ in most cases)

V_2 = maximum applied bias potential

$S_{21}(\omega, V)|_{PS}$ = voltage transmission coefficient of the phase shifter at V bias

$S_{21}(\omega, 0)|_{PS}$ = voltage transmission coefficient of the phase shifter at zero bias.

With ideal 3 dB quadrature coupling, maintained across the octave bandwidth, the relative phase shift would simply be the superposition of the relative phase shifts in the reflection coefficients, ρ_{T_1} and ρ_{T_2}, produced by the reflection terminations of both stages, i.e.:

$$\Delta \angle S_{21}(\omega, V)|_{PS} = \Delta \angle \rho_{T_1}(\omega, V) + \Delta \angle \rho_{T_2}(\omega, V)$$

where

$$\Delta \angle \rho_{T_1}(\omega, V) = \angle\left(\frac{\rho_{T_1}(\omega, V)}{\rho_{T_1}(\omega, 0)}\right)$$

and

$$\Delta \angle \rho_{T_2}(\omega, V) = \angle\left(\frac{\rho_{T_2}(\omega, V)}{\rho_{T_2}(\omega, 0)}\right)$$

where $\rho_{T_{1(2)}}(\omega, V)$ = voltage reflection coefficient of $Z_{T_{1(2)}}$ at V bias and $\rho_{T_{1(2)}}(\omega, 0)$ = voltage reflection coefficient of $Z_{T_{1(2)}}$ at zero bias.

If the hump produced by the first stage is centered below the lowest frequency of the desired frequency range and that produced by the second stage near the highest frequency, then with the appropriate component values the negative gradients of the first stage will compensate for the positive gradients of the second stage, within the desired frequency range. The resulting frequency response will be flat over the desired frequency range, for relative phase shifts up to and exceeding 180°.

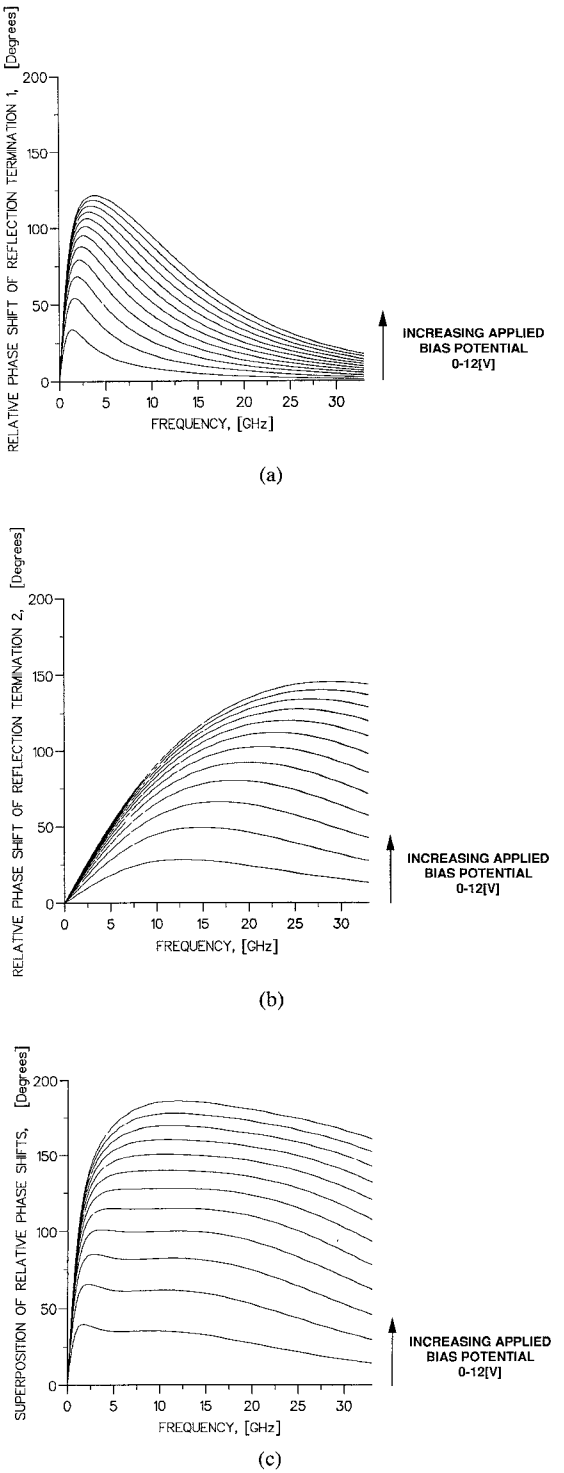

Fig. 3. Relative phase shift for the: (a) reflection coefficient of Z_{T_1}; (b) reflection coefficient of Z_{T_2}; (c) phase shifter with ideal 3 dB quadrature coupling maintained at all frequencies.

Fig. 3 shows the relative phase shift in ρ_{T_1} and ρ_{T_2}, produced by Z_{T_1} and Z_{T_2}, respectively, and the subsequent superposition of these frequency responses for a *Ku*-band CMRTPS, using ideal 3 dB quadrature couplers. Within an octave bandwidth—having a lower band-edge frequency F_1 = 10 GHz, an upper band-edge frequency F_2 = 20 GHz and a mid-band frequency F_O = 15 GHz—the superposition of the frequency responses have negative

gradients. It will be shown in a subsequent design example that the near linear decrease in the isolation, with respect to frequency, of the 4-finger Lange couplers can increase the gradient to its desired zero value.

II. Simulation

The directional coupler can be assumed to be symmetrical, reciprocal and lossless—which is a good approximation in most cases.

Therefore, with the appropriate expressions obtained for a Lange couplers' even mode effective permittivity, $\epsilon_{ee}(f)$; odd mode effective permittivity, $\epsilon_{eo}(f)$; even mode capacitance, $C_{oe}(f)$; odd mode capacitance, $C_{oo}(f)$, and the finger length, l, [15] the 4-port steady-state S-parameters S_{ij} (where $i, j \in [1, 4]$), can be accurately determined [16].

In some circumstances, it may not be possible to cascade the 2-stages of the CMRTPS without some form of matched, lossless, transmission line—due to restricted layout considerations. If this stage isolation line (SIL) is to be inserted between the stages, its model must be included in the simulations.

S-parameters resulting from transient, time-domain, signals can clearly describe the direction of transient power flow around the topology. Using the 4-port steady-state S-parameters of the directional coupler, the transient 2-port S-parameters for the 2-stage CMRTPS, $S_{mn}|_{PS}$ (where $m, n \in [1, 2]$), can be expressed as follows:

$$S_{11}|_{PS} = S_{22}|_{PS} = S_{11A} + (S_{21A}S_{21C})^2 \cdot \sum_{i=0}^{p} S_{11B}^{(i+1)} S_{22A}^{i}$$

$$S_{21}|_{PS} = S_{12}|_{PS} = S_{21A}S_{21C}S_{21B} \cdot \sum_{i=0}^{p} (S_{11B}S_{22A})^{i}$$

where

S_{mnA} = Steady-state S-parameter for the first stage
S_{mnB} = Steady-state S-parameter for the second stage
S_{mnC} = Steady-state S-parameter for the SIL
p = order of inter-stage reflection.

Here,

$$S_{11A(B)} = S_{22A(B)} = S_{11} + (S_{21}^2 + S_{41}^2) \cdot \sum_{i=0}^{q} \rho_{T_{1(2)}}^{(i+1)} S_{11}^{i}$$

$$S_{21A(B)} = S_{12A(B)} = S_{31} + 2S_{21}S_{41} \cdot \sum_{i=0}^{q} \rho_{T_{1(2)}}^{(i+1)} S_{11}^{i}$$

where q = order of intra-stage reflection

$$S_{21C} = e^{-j\theta_c(\omega)}$$

where $\theta_c(\omega)$ = electrical length of the SIL where

$$\theta_c(\omega) = \frac{\omega}{\omega_O} \cdot \theta(\omega_O)$$

and

$$\theta(\omega_O) = \frac{\omega_O \sqrt{\epsilon_e(\omega_O)}}{c} \cdot l_c$$

where ϵ_e = effective permittivity of the SIL and, l_c = physical length of the SIL.

For the true steady-state 2-port S-parameters, both p and q must tend to infinity, resulting in the following closed-form expressions:

$$S_{11}|_{PS} = S_{22}|_{PS} = S_{11A} + \frac{(S_{21A}S_{21C})^2 S_{11B}}{1 - S_{22A}S_{11B}}$$

$$S_{21}|_{PS} = S_{12}|_{PS} = \frac{S_{21A}S_{21C}S_{21B}}{1 - S_{22A}S_{11B}}$$

where

$$S_{11A(B)} = S_{22A(B)} = S_{11} + \frac{\rho_{T_{1(2)}}(S_{21}^2 + S_{41}^2)}{1 - \rho_{T_{1(2)}}S_{11}}$$

and

$$S_{21A(B)} = S_{12A(B)} = S_{31} + \frac{2\rho_{T_{1(2)}}S_{21}S_{41}}{1 - \rho_{T_{1(2)}}S_{11}}.$$

III. Synthesis

In order to synthesize the 2-stage octave bandwidth CMRTPS, the reflection terminations and directional couplers can be treated separately. However, it should be noted that the empirical expressions obtained for the component values within the reflection terminations are a function of the characteristics of the directional couplers and the presence of the other stage.

In theory, it will be seen that the exact frequency characteristics obtained with the CMRTPS covering an octave bandwidth can be scaled to cover any chosen octave bandwidth. This is achieved by the appropriate scaling of the component values within the reflection terminations and the physical length of the directional coupler.

Directional Couplers

Two-stage octave bandwidth CMRTPS's require octave bandwidth directional couplers—with tight coupling within the bandwidth.

In order to achieve a return loss within acceptable levels, 3 dB coupling is required at the frequency of maximum coupling, F_C, —with a 3 dB coupling imbalance, $C_I \leq \pm 1.5$ dB, within the octave bandwidth. Many types of directional coupler qualify, such as the common 4-finger Lange coupler. However, the narrow band 1-section branch line coupler has also been used in wideband RTPS's [7], [8].

Reflection Termination

A single flat level relative phase shift frequency response is quite easy to achieve over an octave bandwidth. As the number of required flat levels increase, the difficulties in achieving these flat levels also increases. In order to obtain a low phase and amplitude error over the full octave bandwidth, at all levels from 0° to over 180°, the following conditions have been found and must be satisfied by the reflection terminations:

a) The resonant frequency of the second stage reflection termination must correctly scale that of the first stage, at the zero bias potential.

b) The change in the resonant frequency of the second stage reflection termination must correctly track the change in that of the first stage.

c) The reflection coefficient of the second stage reflection termination must have a phase angle whose gradient, with respect to frequency, correctly scales that of the first stage, at their respective frequency of resonance.

These conditions will now be examined in detail.

A. Initial Resonance Scaling

At zero bias, linear relationships exist between the resonant frequency of the first and second stage reflection terminations and the mid-band frequency, i.e.:

$$\frac{\omega_{OS_1}(0)}{\omega_O} \equiv A_1 \quad \text{and} \quad \frac{\omega_{OS_2}(0)}{\omega_O} \equiv A_2$$

where

$\omega_{OS_1}(0)$ = series resonant frequency of Z_{T_1} at zero bias
$\omega_{OS_2}(0)$ = series resonant frequency of Z_{T_2} at zero bias
$\omega_O = 2\pi F_O$
A_1 = frequency scaling factor for Z_{T_1}
A_2 = frequency scaling factor for Z_{T_2}.

Therefore,

$$\frac{\omega_{OS_2}(0)}{\omega_{OS_1}(0)} \equiv A_3$$

i.e., initial resonance scaling.

The following design equations can now be obtained:

$$C_{1_T}(0) = \frac{1}{(A_1\omega_O)^2 L_1} \quad \text{and} \quad C_{2_T}(0) = \frac{1}{(A_2\omega_O)^2 L_2}$$

where $C_{1_T}(0)$ = total series capacitance in Z_{T_1} at zero bias and $C_{2_T}(0)$ = total series capacitance in Z_{T_2} at zero bias.

B. Resonance Tracking

The tuning ratio, $m(V)$, of a series resonant tuned circuit is defined as

$$m(V) = \frac{\omega_{OS}(V)}{\omega_{OS}(0)}.$$

Chip varactors have negligible parasitic reactive components below 10 GHz. If chip varactors are employed to vary the resonant frequency, with voltage-invariant series inductors, it can be shown that:

$$m(V) = \sqrt{\frac{C(0)}{C(V)}}$$

where $C(V)$ = junction capacitance of the chip varactor with V bias and $C(0)$ = junction capacitance of the chip varactor with zero bias.

In general, the junction capacitance can be expressed as

$$C(V) = \frac{C(0)}{(1 + V/\phi)^\gamma}$$

where

ϕ = built-in barrier potential
γ = slope exponent.

Therefore,

$$m(V) = \sqrt{(1 + V/\phi)^\gamma}.$$

As $m(V)$ increases, the size of the hump in the relative phase shift frequency response, for a single stage reflection-type phase shifter, also increases. The rate at which this size increases, with respect to an increase in the bias potential, increases as $\omega_{OS}(0)$ increases. Since $\omega_{OS_2}(0) > \omega_{OS_1}(0)$, for a 2-stage CMRTPS, if an identical bias is applied to all varactors the reflection termination of the second stage must incorporate a specific amount of decoupling, in order to reduce the rate in which its peak increases.

The decoupling can be realized by a voltage invariant series coupling capacitor, C_C. This capacitor has the second function of dc blocking—if placed between the reflection termination and the corresponding port of its directional coupler. Dc blocking may be required to isolate the applied bias from the other stage and the input and output ports of the phase shifter.

With the introduction of C_C, the total series capacitance of a reflection termination, $C_T(V)$, is now given by

$$C_T(V) = \frac{C_C C(V)}{C_C + C(V)}.$$

The amount of coupling between the reflection termination and its directional coupler can be expressed by the reflection termination coupling coefficient, k, defined as

$$k = \frac{C_C}{C_C + C(0)}$$

where $k = 0$ for an uncoupled reflection termination and $k = 1$ for a fully coupled reflection termination.

In most cases, the reflection termination of the first stage can be fully coupled. This has the advantage of making the value of C_C, non-critical. As a good rule-of-thumb, make $C_{C_1} \geq 20 \cdot C_1(V)$, therefore, $k_1 \simeq 1$.

If identical technologies and slope exponents are used in the junction capacitances of both stages, i.e., $\phi_1 = \phi_2$

$= \phi$ and $\gamma_1 = \gamma_2 = \gamma$, respectively, it can be shown that when the first stage reflection termination is fully coupled the tuning ratio of Z_{T_2}, $m_2(V)$, is given by

$$m_2(v) = \sqrt{k_2 m_1^2(V) - k_2 + 1}$$

i.e., resonance tracking

where $m_1(V)$ = tuning ratio of Z_{T_1} and

$$m_1(V) = \sqrt{(1 + V/\phi)^{\gamma}}.$$

Therefore,

$$\frac{\partial m_2(V)}{\partial V} = \frac{\gamma k_2 (1 + V/\phi)^{(\gamma - 1)}}{2\phi \sqrt{k_2(1 + V/\phi)^{\gamma} - k_2 + 1}}$$

and

$$\frac{\partial m_1(V)}{\partial V} = \frac{\gamma}{2\phi} (1 + V/\phi)^{((\gamma/2) - 1)}.$$

Therefore,

$$0 \leq \frac{\partial m_2(V)}{\partial V} \leq \frac{\partial m_1(V)}{\partial V}.$$

The lower limit is reached when $k_2 = 0$ and the upper when $k_2 = 1$.

In order to achieve a low phase error at all levels, over an octave bandwidth, it is found that k should be just under 0.5, resulting in $\partial m_2(V)/\partial V \approx \frac{1}{2} \cdot \partial m_1(V)/\partial V$.

C. Phase Gradient Scaling

The reflection coefficient of a reflection termination, ρ_T, is defined as

$$\rho_T = \frac{Z_T - Z_O}{Z_T + Z_O}$$

where Z_T = reflection termination impedance and Z_O = reference impedance standard for the system ($Z_O = 50\ \Omega$, in most cases).

For a series R-L-C reflection termination, the following is obtained:

$$\rho_T = \frac{(R_S^2 - Z_O^2 + X_S^2) + j(2Z_O X_S)}{(R_S + Z_O)^2 + X_S^2}$$

where

$X_S = X_L + X_C$
R_S = total series loss resistance
X_L = reactance of the total series inductance
X_C = reactance of the total series capacitance.

Therefore,

$$|\rho_T| = \sqrt{\left(\frac{(R_S^2 - Z_O^2 + X_S^2)}{(R_S + Z_O)^2 + X_S^2}\right)^2 + \left(\frac{2Z_O X_S}{(R_S + Z_O)^2 + X_S^2}\right)^2}$$

and

$$\angle \rho_T = \tan^{-1}\left(\frac{2Z_O X_S}{R_S^2 - Z_O^2 + X_S^2}\right).$$

Therefore,

$$\frac{\partial \angle \rho_T}{\partial \omega} = -\frac{2Z_O(X_L - X_C)}{\omega} \cdot \left(\frac{2X_S^2 - (R_S^2 - Z_O^2 + X_S^2)}{(2Z_O X_S)^2 + (R_S^2 - Z_O^2 + X_S^2)^2}\right).$$

At resonance:

$$\left.\frac{\partial \angle \rho_T}{\partial \omega}\right|_{\omega OS} = -\frac{4Z_O L}{Z_O^2 - R_S^2} \simeq -\frac{4L}{Z_O},$$

with high-Q chip varactors.

Therefore,

$$\left.\frac{\partial \angle \rho_T}{\partial \omega}\right|_{\omega OS} \equiv K \cdot L,$$ i.e., a constant, irrespective of ω_{OS}

where K = phase gradient constant.

For the 2-stage topology, it is found that a linear relationship must exist between the angle of reflection coefficient gradients, at their respective resonant frequencies, i.e.:

$$\frac{\partial \angle \rho_{T_1}/\partial \omega|_{\omega OS_1}}{\partial \angle \rho_{T_2}/\partial \omega|_{\omega OS_2}} \equiv A_4,$$ i.e., phase gradient scaling.

Therefore, the following relationship can be obtained:

$$L_1 = \left(A_4 \frac{K_2}{K_1}\right) L_2 \simeq A_4 L_2,$$

with high-Q chip varactors and identical directional couplers where K_1 = phase gradient constant for Z_{T_1} and K_2 = phase gradient constant for Z_{T_2}.

In order to achieve a low phase error, at all levels over an octave, or greater, bandwidth, it is found that $|\partial \angle \rho_{T_2}/\partial \omega|_{\omega OS_2}$ must be less than $|\partial \angle \rho_{T_1}/\partial \omega|_{\omega OS_1}$, i.e., $A_4 > 1$.

As A_4 is increased beyond unity, the potential bandwidth continues to increase and the rate in which the peak increases effectively decreases in the second stage of the CMRTPS. The latter is similar to reflection termination decoupling.

It has also been found that a linear relationship exists between $\partial \angle \rho_{T_1}/\partial \omega|_{\omega OS_1}$ and ω_O. It follows that linear frequency scaling of L_1 and therefore, L_2 can be performed, i.e.:

$$L_1 = \frac{A_5}{F_O} \quad \text{and} \quad L_2 = \frac{A_6}{F_O}.$$

Octave Bandwidth Design

Numerous 2-stage octave bandwidth CMRTPS's have been simulated using 4-finger Lange couplers—on a 25

mil thick alumina substrate, having a dielectric constant, $\epsilon_r = 9.8$.

The physical length of the Lange coupler dictates its frequency of maximum coupling, F_C. In order to obtain the optimum performance over the octave bandwidth, F_C is set slightly higher than the mid-band frequency. The reason for this increase will be discussed later.

Values for the previously defined empirical constants: A_1; A_2; A_5; A_6; k_1 and k_2 have been found which result in a phase error of less than $\pm 2.4°$ and a maximum amplitude error of less than ± 0.21 dB over the complete octave bandwidth—for relative phase shift levels up to and exceeding 180°.

These values are given in Table I. It should be noted that these values apply only to the type of directional coupler and substrate defined previously.

Quick design equations, based on the above tabulated values, are given below:

$$L_1 = \frac{3.9}{F_O}; \quad C_1(0) = \frac{48}{F_O}; \quad C_{C_1} > \frac{960}{F_O}$$

$$L_2 = \frac{2.55}{F_O}; \quad C_2(0) = \frac{8.55}{F_O}; \quad C_{C_2} = \frac{13.5}{F_O}$$

and

$$F_C = 1.087 F_O$$

where L has units of [nH]; C has units of [pF]; F_O has units of [GHz].

Ku-Band Example

The following example of a 2-stage *Ku*-Band CMRTPS, with a mid-band frequency of 15 GHz, will serve to illustrate the above design techniques. The complete circuit diagram for a 2-stage CMRTPS, without a SIL is illustrated in Fig. 4. The component values for the reflection terminations and the finger dimensions for the 4-finger Lange couplers are given in Table II.

The following empirical expressions for $\epsilon_{ee}(f)$, $\epsilon_{eo}(f)$, $C_{oe}(f)$ and $C_{oo}(f)$ have been determined for the 4-finger Lange coupler, based on the results of Childs [15]:

$$\epsilon_{ee}(f) = 6.476 + 2.995 * 10^{-2} f + 8.469 * 10^{-4} f^2 - 1.739 * 10^{-5} f^3$$

$$\epsilon_{eo}(f) = 5.351 - 9.814 * 10^{-4} f - 1.976 * 10^{-4} f^2 + 4.317 * 10^{-6} f^3$$

$$C_{oe}(f) = 75.352 + 8.883 * 10^{-2} f + 1.2269 * 10^{-3} f^2 + 6.625 * 10^{-6} f^3$$

$$C_{oo}(f) = 399.28 - 6.323 * 10^{-2} f - 1.715 * 10^{-2} + 5.707 * 10^{-4} f 3 - 4.777 * 10^{-6} f^4$$

where C_{oe} and C_{oo} are in [pF] and f is in [GHz]. The above expressions are valid for frequencies up to 33 GHz.

TABLE I
EMPIRICAL CONSTANTS FOR THE OCTAVE BANDWIDTH DESIGN

A_1	A_2	A_5	A_6	k_1	k_2
0.368	1.1348	3.900	2.550	>0.950	0.388

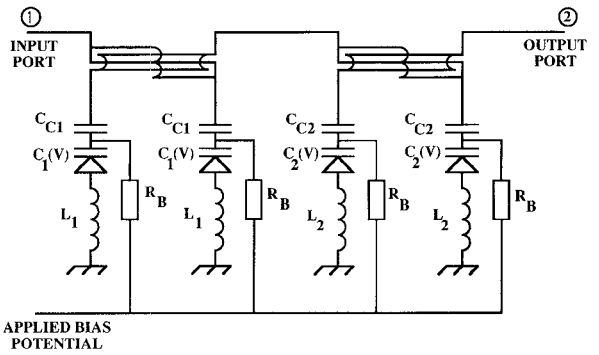

Fig. 4. Complete circuit of a 2-stage cascaded-match reflection-type phase shifter.

The resulting power and phase characteristics for the coupler are shown in Fig. 5. These characteristics are identical to those obtained using EESOF's "Touchstone" package.

The simulated frequency responses for this CMRTPS, using GaAs chip varactors (with $\gamma = 1.0$); $R_{S_1} = R_{S_2} = 0.5\ \Omega$ and $Z_O = 50\ \Omega$, are shown in Fig. 6.

With reference to Figs. 3(c), 5 and 6(a), the negative gradients in Fig. 3(c) have been compensated for, within the octave bandwidth.

As frequency decreases below F_1 or increases above F_2, $\Delta \angle S_{21}|_{PS}$ begins to increase from its level state. This is the result of the higher-order inter-stage reflections becoming more significant—as the return losses at port 2 of RTPS-1 and port 1 of RTPS-2 decrease—due to the increase in the 3 dB coupling imbalance.

Eventually, a point is reached where $(\partial \Delta \angle S_{21}/\partial \omega)|_{PS} \equiv 0$, beyond which the decrease in the power coupling of the directional coupler dominates. With less reflected power emerging from port 2 of RTPS-1—and, therefore, RTPS-2—the $\Delta \angle S_{21}|_{PS}$ response begins to rapidly decrease. The two resulting peaks must be located well away from octave band edges, as the changing gradients of their skirts are difficult to predict and, therefore, control.

With the types of directional couplers and substrates defined previously, the first peak is centered at approximately 0.31 F_C; while the second peak is at approximately 1.67 F_C. The second peak is much greater in amplitude, compared to the first peak, due to the decreased isolation at that peak.

It has been found that the range of maximum $\Delta \angle S_{21}|_{PS}$ flatness has a centre located just below F_C. This is because the decrease in isolation, as frequency increases, causes the 3 dB coupling imbalance to increase more at $F_C + \Delta F_C$ then at $F_C - \Delta F_C$, where ΔF_C is a small frequency offset from F_C. Therefore, in order to obtain the maximum

TABLE II
COMPONENT VALUES AND FINGER DIMENSIONS FOR THE *Ku*-BAND EXAMPLE

L_1 [nH]	$C_1(0)$ [pF]	C_{C1} [pF]	L_2 [nH]	$C_2(0)$ [pF]	C_{C2} [pF]	Length [μm]	Width [μm]	Separation [μm]
0.26	3.2	>64	0.17	0.57	0.9	1850	65	53

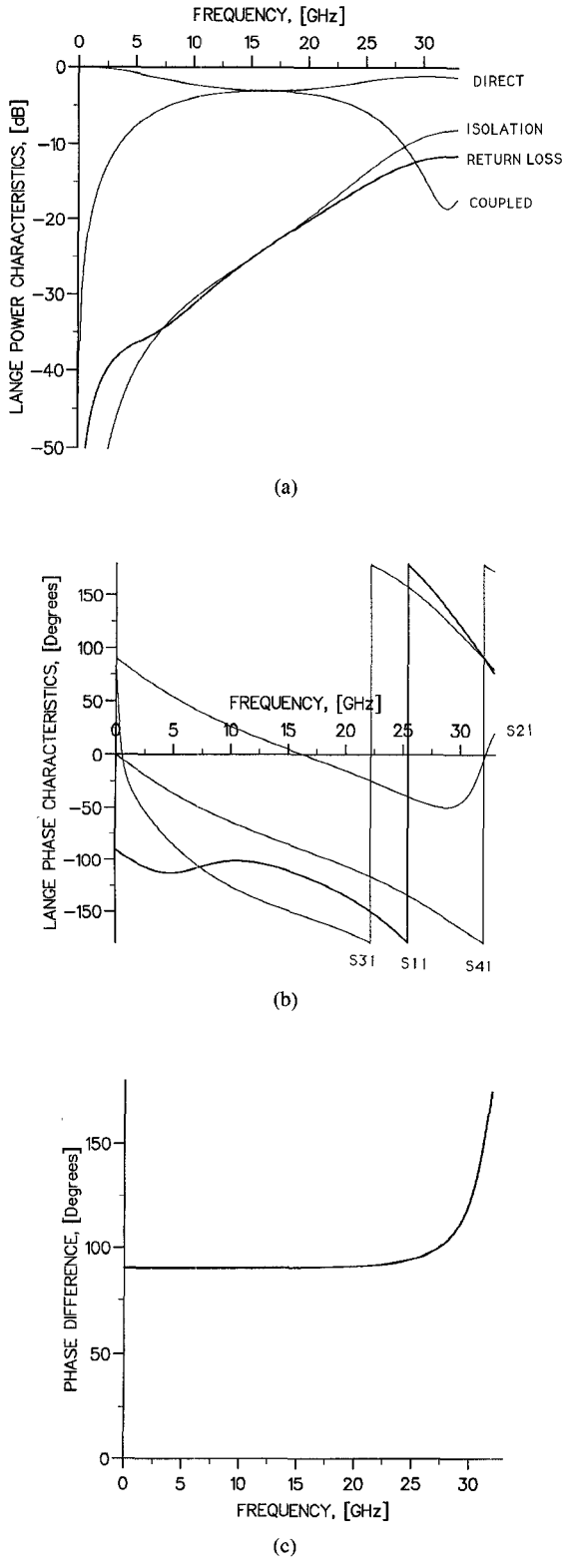

Fig. 5. Four-finger Lange coupler characteristics. (a) Power. (b) Phase. (c) Phase difference between the coupled and direct port signals.

bandwidth, the mid-band frequency should be negatively offset slightly from F_C, i.e., $F_O \simeq 0.85\ F_C$ with the type of directional coupler and substrate defined previously.

For the octave bandwidth design presented here, an offset of $F_C = 1.087\ F_O$ was found to provide the minimum error in both the phase and amplitude and maximum return loss across the bandwidth.

A complete breakdown in the $\Delta \angle S_{21}|_{PS}$ response is found around $1.72\ F_C$. This is due to the rapid increase in deviation from phase quadrature, as seen in Fig. 5(c).

IV. DISCUSSION

In order to realize the design of the 2-stage octave bandwidth CMRTPS, the tuning requirements of the CMRTPS and the varactor technologies available must be considered. Only varactors with a mesa type construction will be considered in detail, as accurate high-frequency models for planar MESFET type varactors are not available.

Varactor-type devices can be categorized by the semiconductor material from which they are made and by their doping profiles. Devices made from silicon have a barrier potential, $\phi = 0.7 - 0.8$ V, while GaAs have $\phi = 1.2 - 1.3$ V. In general, the Q-factor of a GaAs device is approximately four times that of an equivalent silicon device. As a result, the phase shifter would have a much better insertion loss performance if GaAs varactors were employed. Q-values in excess of 75, at 10 GHz, are commercially available for GaAs chip varactors with a $C(4\text{ V}) = 0.5$ pF junction capacitance and a total series resistance, $R_{SV}(4\text{ V}) = 0.42\ \Omega$.

The total series resistance of a mesa type varactor is the result of: an undepleted epitaxial region resistance, Ohmic contact resistance, spreading resistance between the epitaxial and substrate layers, and the substrate layer resistance. The undepleted epitaxial region resistance is a function of the applied bias potential. When the undepleted epitaxial region decreases, due to increases in the applied bias potential, $R_{SV}(V)$ decreases. Since the total series resistance of the varactor makes-up the bulk of the total series resistance of the reflection termination, $R_S(V)$ also decreases.

The simulations in the previous section have assumed a voltage-invariant R_S. However, with state-of-the-art high-Q GaAs varactors, this is a good approximation, for most applications.

A device with $\gamma = 0.5$ is defined as having an abrupt junction (AJ), while those with $\gamma > 0.5$ are defined as having a hyper-abrupt junction (HAJ). The value of γ depends on the doping profile of the active layer. Traditionally, HAJ devices have voltage dependant γ values. How-

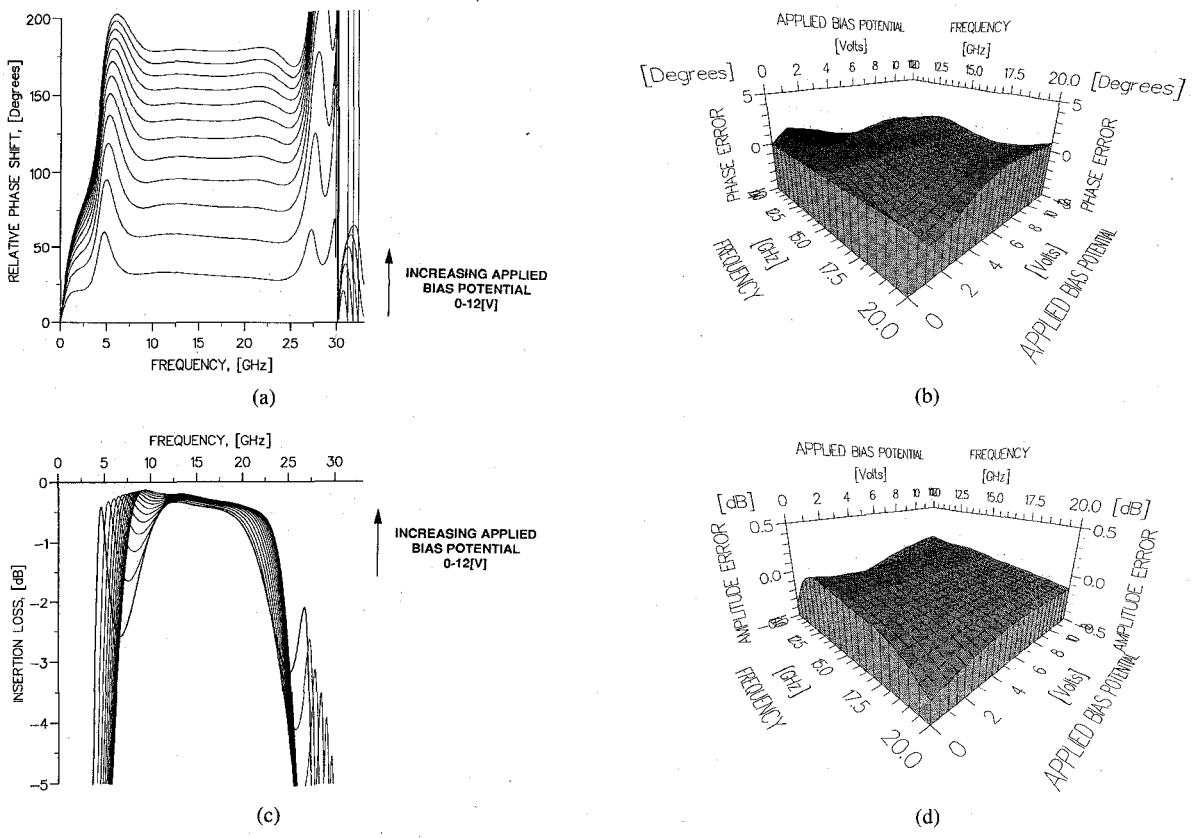

Fig. 6. Simulated performance of a 2-stage *Ku*-band CMRTPS. (a) Relative phase shift. (b) Phase error. (c) Insertion loss. (d) Amplitude error.

ever, constant-γ varactors are now commercially available. In general, the Q-factor of a HAJ varactors is approximately a factor of 2 to 3 higher than equivalent AJ varactors.

The tuning curve of the 2-stage octave bandwidth CMRTPS is given in Fig. 7. From Fig. 7, the $\Delta \angle S_{21}|_{PS} - V$ tuning characteristics for various types of varactor are shown in Fig. 8. It can be deduced from Fig. 7 and seen in Fig. 8 that near linear tuning can be achieved, without any form of bias equalization network, with HAJ varactors having $\gamma = 2.0$.

Since the breakdown voltage, V_B, of most varactor devices is less than 40[V], it will be apparent, from Fig. 8, that only constant-γ GaAs HAJ varactors will be suitable for achieving the 180° level of relative phase shift. If AJ varactors are to be employed, a wideband 90° binary phase shifter could be added to achieve the 180° level, resulting in a slight performance degradation.

Assuming $(V_B - V_2) \geq (\phi + V_1)$, if the RF power level exceeds a critical saturation value, $P_{\mathrm{MAX}}(V)$, forward bias rectification occurs and unwanted harmonics will be generated. For a 3 dB directional coupler and a 3 dB coupling imbalance of ± 1.5 dB, the value of $P_{\mathrm{MAX}}(V)$ is given as

$$P_{\mathrm{MAX}}(V) = \frac{0.354}{Z_O} \cdot (\phi + V)^2 \quad \text{for } -\phi \leq V \leq (V_B - \phi)/2.$$

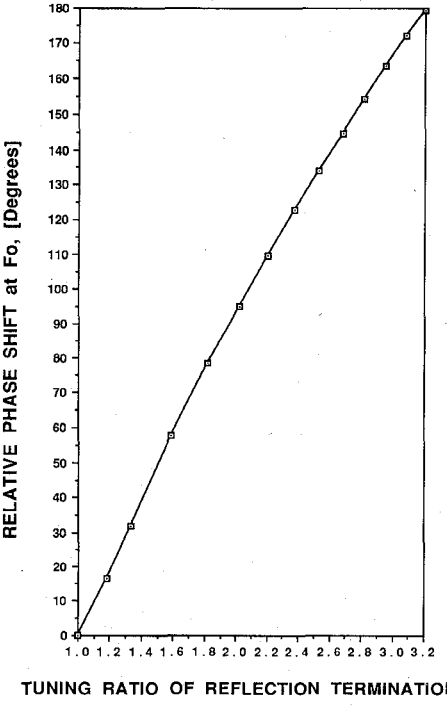

Fig. 7. Tuning curve for the 2-stage octave bandwidth CMRTPS.

Therefore, $P_{\mathrm{MAX}}(V)$ decreases as V decreases. For a 50 Ω system with V_1 set to zero: $P_{\mathrm{MAX}}(V_1) = 10.7$ dBm for GaAs varactors and $P_{\mathrm{MAX}}(V_1) = 5.4$ dBm for Si varac-

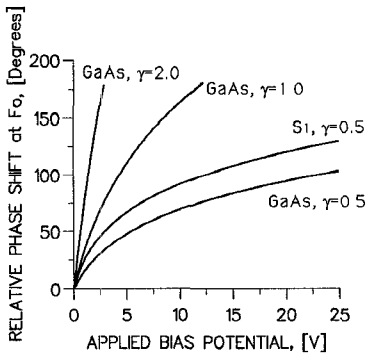

Fig. 8. $\Delta \angle S_{21}|_{PS} - V$ tuning characteristics for various types of varactor.

tors. If the RF power level is to exceed $P_{MAX}(V_1)$, with a hybrid realization, the value of V_1 must be increased to

$$V_1 = \left(\frac{Z_O P_{MAX}(V_1)}{0.354}\right)^{1/2} - \phi$$

An increase in V_1, from zero, will force a subsequent increase in V_2, in order to achieve the 180° level—resulting in an increased performance degradation at the higher levels.

For a hybrid realization of the CMRTPS, Mesa-type varactors are generally used. Here, the parasitics associated with the chip varactors have a significant effect on the performance of the CMRTPS above 10 GHz. With the *Ku*-band design example, a factor of 2 degradation in the ideal phase error was found.

At present, a MMIC realization of the CMRTPS would generally use planar-type varactors. Here, varactors can be realized by connecting together the drain and source terminations of a standard MESFET—resulting in a single Schottky junction. The bias potential is then applied across the drain/source and gate terminations. An MMIC RTPS using this technique has been reported by Bianchi *et al.* [12].

MMIC varactors, resulting in large tuning ratios, can be produced using selective ion implantation (SII) techniques to nonuniformly dope the active region. At present, SII is comparatively a very expensive operation. However, a number of RTPS's have been reported using these devices [6], [8], [9].

The small parasitic reactances associated with MMIC varactors should result in a negligible degradation in the ideal phase error of the *Ku*-band design example.

V. Conclusion

The novel technique of cascading matched RTPS's has been presented. With the three conditions for the reflection terminations satisfied, the bandwidth limitations of the nonideal 4-finger Lange coupler can be overcome to realize high performance octave bandwidth 180° analog phase shifters.

With high-Q GaAs HAJ varactors, the CMRTPS can achieve the 180° relative phase shift level with a low applied bias potential and exhibit excellent insertion loss and noise figure characteristics.

Due to the inherently small, yet well characterized, parasitics associated with a MMIC realization and with a good design layout, the measured performance should be close to that predicted.

The linear transmission phase and error characteristics make the 2-stage CMRTPS ideally suited for low power wide-band oscillators and beam forming network applications.

References

[1] R. N. Hardin, E. J. Downey, and J. Munushian, "Electronically—variable phase shifters utilizing variable capacitance diodes," *Proc. IRE*, vol. 48, pp. 944–945, May 1960.

[2] R. M. Searing, "Variable capacitance diodes used as phase shift devices," *Proc. IRE*, vol. 49, pp. 640–641, Mar. 1961.

[3] R. V. Garver, "Broadband binary 180° diode phase modulator," *IEEE Trans. Microwave Theory Tech.*, vol. MTT-13, pp. 32–38, Jan. 1965.

[4] B. T. Henoch and P. Tamm, "A 360° reflection-type diode phase modulator," *IEEE Trans. Microwave Theory Tech.*, vol. MTT-19, pp. 103–105, Jan. 1971.

[5] B. Ulriksson, "Continuous varactor-diode phase shifter with optimized frequency response," *IEEE Trans. Microwave Theory Tech.*, vol. MTT-27, pp. 650–654, July 1979.

[6] D. E. Dawson, A. L. Conti, S. H. Lee, G. F. Shade, and L. E. Dickens, "An analog X-band phase shifter," in *1985 IEEE Microwave and Millimeter-Wave Monolithic Circuits Symp. Dig.*, pp. 6–10.

[7] E. C. Niehenke, V. V. DiMarco, and A. Friedberg, "Linear analog hyperabrupt varactor diode phase shifters," in *1985 IEEE MTT-S Int. Microwave Symp. Dig.*, pp. 657–660.

[8] C. L. Chen, W. E. Courtney, L. J. Mahoney, L. J. Manfra, A. Chu, and H. A. Atwater, "A low-loss Ku-band monolithic analog phase shifter," *IEEE Trans. Microwave Theory Tech.*, vol. MTT-35, pp. 315–320, Mar. 1987.

[9] D. M. Krafcsik, S. A. Tmhoff, D. E. Dawson, and A. L. Conti, "A dual-varactor, analog phase shifter operating 6 to 18 GHz," in *1988 IEEE Microwave and Millimeter-Wave Monolithic Circuits Symp. Dig.*, pp. 83–86.

[10] J. I. Upshur and B. D. Geller, "Low-loss 360° X-band analog phase shifter," in *1990 IEEE MTT-S Int. Microwave Symp. Dig.*, pp. 487–490.

[11] P. Miller and J. S. Joshi, "MMIC phase shifters for space applications," *ESA/ESTEC Proc. Int. Workshop on Monolithic Microwave Integrated Circuits for Space Applications*, Mar. 1990.

[12] G. Bianchi, G. Pinto, and C. Giuliani, "MMIC 12-13 GHz voltage controlled phase shifter," *ESA/ESTEC Proc. Int. Workshop on Monolithic Microwave Integrated Circuits for Space Applications*, Mar. 1990.

[13] S. Hara, T. Tokumitsu and M. Aikawa, "Lossless, broadband monolithic microwave active inductors," in *1989 IEEE MTT-S Int. Microwave Symp. Dig.*, pp. 955–958.

[14] E. M. Bastida, G. P. Donzelli, and L. Scopelliti, "GaAs monolithic microwave integrated circuits using broadband tunable active inductors," in *Proc. 19th European Microwave Conf.*, Sept. 1989, pp. 1282–1287.

[15] W. H. Childs, "A 3-dB Interdigitated Coupler on Fused Silica," in *1977 IEEE MTT-S Int. Microwave Symp. Dig.*, pp. 370–372.

[16] ——, "Microstrip directional couplers," Mullard Technical Communications, No. 116, pp. 177–189, Oct. 1972.

Stepan Lucyszyn (M'91) was born in Bradford, England, in 1965. He received the honours degree in electronic and communications engineering from the Polytechnic of North London, England, in 1987. At his graduation he was awarded the departmental prize. In 1988 he received the masters degree in satellite communication engineering from the University of Surrey, England.

He then spent a year in the space industry, as a Communication Systems Engineer. Since 1989 he has been with the Communications Research Group at King's College, University of London, studying towards the Ph.D. in Microwave Engineering. His research interests include the design, realization, measurement and characterization of novel MMIC devices.

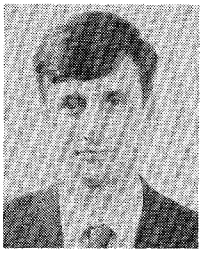

Ian D. Robertson (M'91) was born in 1963 in London, England. He graduated from King's College, University of London, in 1984 with a first class honours degree in electrical and electronic engineering. He was awarded the Siemens Prize and the IEE Prize for academic achievement in his final year.

From 1984 to 1986 he was employed at Plessey Research (Caswell) in the GaAs MMIC Research Group, where he worked on MMIC mixers, RF-on-wafer measurement component design, and FET characterization. From 1986 to 1990 he was employed as a research assistant at King's College, and studied part-time on Ph.D. research into MMIC mixers. He is currently a Lecturer at King's College, and leads the MMIC Research team in the Communications Research Group.